

OASI: Objective-Aware Surrogate Initialization for Multi-Objective Bayesian Optimization in TinyML Keyword Spotting

Soumen Garai, and Suman Samui *Member, IEEE*,

Department of Electronics and Communication Engineering,

National Institute of Technology Durgapur, West Bengal 713209, India

Abstract—Voice assistants utilize Keyword Spotting (KWS) to enable efficient, privacy-friendly activation. However, realizing accurate KWS models on ultra-low-power TinyML devices (often with less than < 2 MB of flash memory) necessitates a delicate balance between accuracy with strict resource constraints. Multi-objective Bayesian Optimization (MOBO) is an ideal candidate for managing such a trade-off but is highly initialization-dependent, especially under the budgeted black-box setting. Existing methods typically fall back to naive, ad-hoc sampling routines (e.g., Latin Hypercube Sampling (LHS), Sobol sequences, or Random search) that are adapted to neither the Pareto front nor undergo rigorous statistical comparison. To address this, we propose Objective-Aware Surrogate Initialization (OASI), a novel initialization strategy that leverages Multi-Objective Simulated Annealing (MOSA) to generate a seed Pareto set of high-performing and diverse configurations that explicitly balance accuracy and model size. Evaluated in a TinyML KWS setting, OASI outperforms LHS, Sobol, and Random initialization, achieving the highest hypervolume (0.0627) and the lowest generational distance (0.0) across multiple runs, with only a modest increase in computation time (1934 s vs. ~ 1500 s). A non-parametric statistical analysis using the Kruskal-Wallis test ($H = 5.40$, $p = 0.144$, $\eta^2 = 0.0007$) and Dunn's post-hoc test confirms OASI's superior consistency despite the non-significant overall difference with respect to the $\alpha = 0.05$ threshold.

Index Terms—Multi-objective optimization, Bayesian optimization, Initialization methods, Keyword spotting, TinyML

I. INTRODUCTION

Speech assistants such as Amazon Echo and Google Home have become part of daily life. Yet, sending audio streams continuously to the cloud creates problems of network overload, latency, and privacy risks [1]. A common solution is hybrid processing: a lightweight on-device Keyword Spotting (KWS) module detects trigger words (e.g., “Alexa”) before activating cloud-based Automatic Speech Recognition (ASR) system. This reduces communication overhead, but also places strict limits on model size (typically < 2 MB) and computation. TinyML [2] addresses these constraints by enabling efficient and privacy-preserving inference directly on edge devices.

Many works improve KWS by designing compact architectures, using neural architecture search, or applying model compression techniques such as pruning, quantization, and knowledge distillation [3]. While effective, these are usually single-objective methods that yield a single solution. In practice, TinyML KWS requires balancing multiple objectives: maximizing accuracy while minimizing memory, latency, and energy. Multi-objective Bayesian Optimization (MOBO) [4] is well suited for this task, as it builds surrogates of accuracy-efficiency trade-offs and searches for Pareto-optimal solutions.

MOBO's performance is highly sensitive to initialization, which is especially critical under tight evaluation budgets. The prior works on structured sampling methods such as LHS, Sobol, or factorial designs, along with meta-learning approaches like MI-SMBO [?], provide broad early coverage with minimal overhead. Yet, their

objective-agnostic seeds often yield weaker surrogates and slower convergence [4]. In TinyML, these strategies have been applied in an ad-hoc manner, with few systematic comparisons or rigorous statistical evaluations [6].

To address this, we propose **Objective-Aware Surrogate Initialization (OASI)**, a method that uses Multi-Objective Simulated Annealing (MOSA) to generate balanced seed points for MOBO.

Our contributions are as follows:

- We introduce **OASI**, a MOSA-based initialization scheme for MOBO that explicitly balances accuracy and model size in TinyML KWS.
- We integrate OASI into a full MOBO pipeline covering mixed search spaces and realistic deployment constraints.
- We perform head-to-head comparisons with LHS, Sobol, and Random initialization under strict evaluation budgets.
- We adopt non-parametric statistical tests (Kruskal-Wallis, Dunn's) to validate significance and consistency of improvements.

II. PROBLEM DEFINITION AND BACK GROUND

A. Keyword Spotting Pipeline

A continuous audio waveform $x(t)$ is first transformed into frame-wise spectro-temporal features using the Short-Time Fourier Transform (STFT) followed by log-Mel filtering [1], producing

$$E = \{e_0, \dots, e_{T-1}\} \in \mathbb{R}^{T \times K}, \quad (1)$$

where each frame $e_t \in \mathbb{R}^K$. For frame index i , a contextual input slice is constructed as

$$E[i] = [e_{i-s-P}, \dots, e_{i-s}, \dots, e_{i-s+F}] \in \mathbb{R}^{K \times (P+F+1)}, \quad (2)$$

with s denoting stride, P past frames, and F future frames.

An acoustic model g_θ maps each slice to a posterior probability vector:

$$g_\theta(E[i]) = [p(C_1 | E[i]), \dots, p(C_N | E[i])]^\top, \quad (3)$$

where θ are the model parameters, optimized via a supervised loss such as cross-entropy.

Robust detection is obtained through temporal smoothing. For class n , the smoothed posterior at time t is

$$\bar{y}_n(t) = \frac{1}{T} \sum_{i=t-T+1}^t y_n(i), \quad (4)$$

and a keyword event is triggered whenever $\bar{y}_{kw}(t) \geq \tau$ with τ as the detection threshold.

B. Constrained MOO for TinyML

The core computational burden and performance of KWS pipeline is determined by the acoustic model g_θ . Deploying g_θ on TinyML devices requires a highly efficient architecture parameterized by hyperparameters $h \in \mathcal{H}$ [1], [7]. The process of finding the optimal h is formalized as a bi-level, black-box constrained multi-objective optimization problem (C-MOOP).

Let $\mathcal{D} = \{(x_i, y_i)\}_{i=1}^N$ denote the dataset, which is divided into training (\mathcal{D}_{tr}), validation (\mathcal{D}_{val}), and test (\mathcal{D}_{te}) splits. A model is specified by a set of hyperparameters $h \in \mathcal{H}$ and a set of trainable parameters $\theta \in \Theta$. For a fixed hyperparameter configuration h , the model parameters are obtained by solving the training problem

$$\theta^*(h) \in \arg \min_{\theta} \mathcal{L}(\mathcal{D}_{\text{tr}}; \theta, h), \quad (5)$$

where \mathcal{L} denotes the empirical loss function, typically a sum or average over the training examples (e.g., cross-entropy loss). The use of \in reflects that the minimizer may not be unique due to the non-convex nature of neural network training.

Once trained, the model is evaluated on the validation set to compute multiple objectives. Given trained parameters $\theta^*(h)$, the predicted class for an input x is

$$\hat{y}(x; h) = \arg \max_{c \in \mathcal{C}} g_c(x; \theta^*(h), h), \quad (6)$$

where $g_c(\cdot)$ denotes the model output probability for class $c \in \mathcal{C}$. In this work, we focus on two criteria:

$$\text{Acc}(h) = \mathbb{E}_{(x, y) \sim \mathcal{D}_{\text{val}}} [\delta(\hat{y}(x; h), y)], \quad (7)$$

$$\text{Size}(h) = \text{bytes}(\theta^*(h), h), \quad (8)$$

where $\delta(a, b)$ is the Kronecker delta, equal to 1 if $a = b$ and 0 otherwise. $\text{Acc}(h)$ and $\text{bytes}(\cdot)$ represent accuracy and the memory footprint of the trained model.

Computing a hyperparameter configuration h value is expensive, as it requires solving a non-convex lower-level training problem to convergence. Moreover, the search space \mathcal{H} is typically structured and discrete (e.g., layer type, number of filters), making the overall process a black-box combinatorial optimization problem: the objectives $f_1(h)$ and $f_2(h)$ cannot be calculated with a closed-form expression but only with costly training and validation. We then frame the HPO problem as a bi-objective search:

$$\min_{h \in \mathcal{H}} (f_1(h), f_2(h)), \quad (9)$$

where $f_1(h) = -\text{Acc}(h)$ and $f_2(h) = \text{Size}(h)$. Alternatively, a scalarized form may be used as:

$$J(h) = \min_{h \in \mathcal{H}} \lambda f_1(h) + (1 - \lambda) f_2(h), \quad \lambda \in [0, 1]. \quad (10)$$

In either case, each evaluation requires solving the lower-level training problem to obtain $\theta^*(h)$, defining a Bi-Level Multi-Objective Optimization (BL-MOP) problem. The aim is to identify the Pareto set \mathcal{P}^* such that no solution is dominated in both objectives.

The optimization proceeds shown in Figure 1, is an iterative under a fixed evaluation budget T , as outlined in Algorithm 1. The general procedure involves the following core steps for each iteration t : (1) sampling a candidate hyperparameter configuration h_t , (2) solving the lower-level gradient based loss minimization problem (training algorithm) to obtain $\theta^*(h_t)$, and (3) evaluating the upper-level objectives $f(h_t)$ on the validation set. The specific strategy for sampling new candidates (based on a given method) defines the update rule for the search distribution \mathcal{Q}_t . After the budget is exhausted, the final approximation of the Pareto front \mathcal{P}_T is extracted from the archive \mathcal{A} of all evaluated configurations. Each evaluation of h entails training to obtain $\theta^*(h)$ and computing $(\text{Acc}(h), \text{Size}(h))$. Under a budget of T evaluations, the optimizer is expected to return an approximation $\mathcal{P}_T \subset \mathcal{F}$ to the Pareto set/front.

III. PROPOSED OASI FOR MOBO

MOBO [9] is a suitable method for dealing with the constricted multi-objective problem inherent in designing TinyML KWS acoustic models [7]. Search is carried out simultaneously to maximize validation accuracy $f_1(h) = \text{Acc}(h)$ and minimize resources such as model size $f_2(h) = \text{Size}(h)$, with such constraints.

The design vector $h = L, F, K, S, D, B, U$ encodes architectural hyperparameters, including convolutional depth (L), per-layer filters

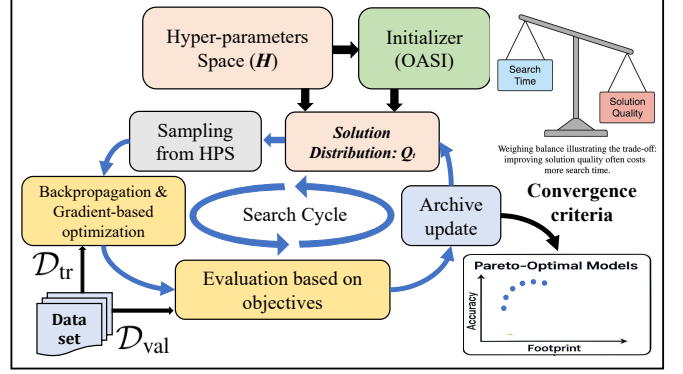


Fig. 1: Block diagram of the bi-level multi-objective optimization process: sampling, training, evaluation, archiving, and Pareto front extraction.

Algorithm 1 Bi-Level Multi-Objective HPO for TinyML

Require: Search space \mathcal{H} ; datasets $\mathcal{D}_{\text{tr}}, \mathcal{D}_{\text{val}}$; budget T
Ensure: Approximated Pareto front \mathcal{P}_T
1: $\mathcal{A} \leftarrow \emptyset$ (archive of evaluated points)
2: **for** $t = 1$ **to** T **do**
3: Sample $h_t \sim \mathcal{Q}_t$
4: $\theta^*(h_t) \leftarrow \arg \min_{\theta} \mathcal{L}(\mathcal{D}_{\text{tr}}; \theta, h_t)$ (lower-level training)
5: $f(h_t) \leftarrow (-\text{Acc}(\mathcal{D}_{\text{val}}; \theta^*(h_t), h_t), \text{Size}(\theta^*(h_t), h_t))$
6: $\mathcal{A} \leftarrow \mathcal{A} \cup \{(h_t, f(h_t))\}$
7: Update \mathcal{Q}_{t+1} given \mathcal{A} (e.g., BO, EA, random)
8: **end for**
9: $\mathcal{P}_T \leftarrow \text{NonDominated}\{f(h) \mid (h, f(h)) \in \mathcal{A}\}$
10: **return** \mathcal{P}_T

(F), kernel sizes (K), strides (S), dropout rates (D), batch normalization flags (B), and dense units (U). For a given configuration h , a model instance M_h is trained with parameters θ on the training set \mathcal{D}_{tr} , yielding optimized weights $\theta^*(h) \in \arg \min_{\theta} \mathcal{L}(\mathcal{D}_{\text{tr}}; \theta, h)$. Because each evaluation requires full training and subsequent validation on \mathcal{D}_{val} , the process is computationally expensive. MOBO alleviates this cost by fitting Gaussian process (GP) surrogates for

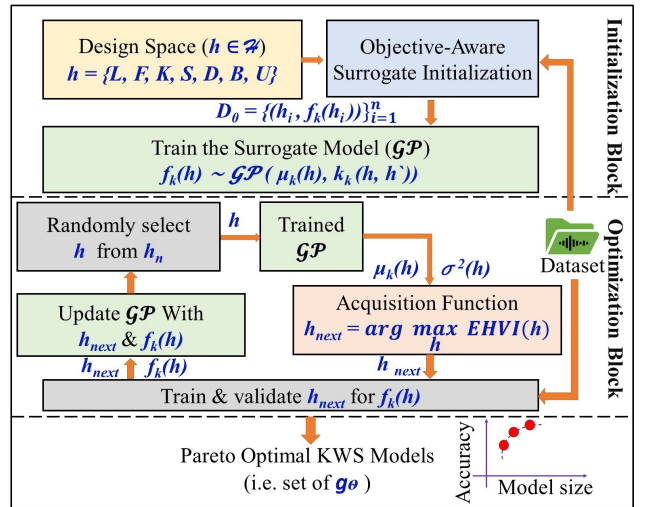


Fig. 2: MOBO framework with proposed OASI framework: MOSA-based initialization with GP-surrogate MOBO for Pareto-optimal KWS models

TABLE I: Sampling methods: description, advantages, and limitations.

Method	Description	Advantages	Limitations
LHS [5]	Divides each parameter range into equal-probability intervals; samples one point per interval.	Good space-filling for small budgets; lower variance than random sampling.	Degrades in high dimensions with few samples.
Random [8]	Samples points independently and uniformly across the design space.	Simple, assumption-free, widely applicable.	Uneven coverage; important regions may be missed.
Sobol [8]	Generates low-discrepancy (quasi-random) sequences for uniform spread.	Deterministic, reproducible, uniform coverage across many sizes.	Best uniformity needs specific sample counts; less effective for very small sets.
Proposed OASI	Simulated annealing-based, objective-aware seeding that emphasizes accuracy-size tradeoffs.	Provides Pareto-focused coverage; robust, repeatable initialization under tight budgets.	Adds slight computational overhead; gains diminish with large budgets.

Algorithm 2 Objective-Aware Surrogate Initialization (OASI)

Require: Search space \mathcal{H} ; objective vector $\mathbf{f}(h)$; number of chains N_{chains} ; iterations per chain N_{iter} ; initial temperatures T_{acc}^0 , T_{size}^0 ; cooling rates α_{acc} , α_{size} ; dataset size n

Ensure: Initial surrogate dataset D_0

- 1: $I_A \leftarrow \emptyset$
- 2: **for** $c = 1$ **to** N_{chains} **do**
- 3: $T_{\text{acc}} \leftarrow T_{\text{acc}}^0$, $T_{\text{size}} \leftarrow T_{\text{size}}^0$
- 4: $h_{\text{curr}} \leftarrow \text{RandomSample}(\mathcal{H})$, $\mathbf{f}_{\text{curr}} \leftarrow \mathbf{f}(h_{\text{curr}})$
- 5: $I_A \leftarrow I_A \cup \{(h_{\text{curr}}, \mathbf{f}_{\text{curr}})\}$
- 6: **for** $i = 1$ **to** N_{iter} **do**
- 7: $h_{\text{next}} \leftarrow \text{Perturb}(h_{\text{curr}})$, $\mathbf{f}_{\text{next}} \leftarrow \mathbf{f}(h_{\text{next}})$
- 8: $I_A \leftarrow I_A \cup \{(h_{\text{next}}, \mathbf{f}_{\text{next}})\}$
- 9: Compute p_{acc} , p_{size} ; sample $u_1, u_2 \sim \mathcal{U}(0, 1)$
- 10: **if** $u_1 < p_{\text{acc}} \wedge u_2 < p_{\text{size}}$ **then**
- 11: $h_{\text{curr}}, \mathbf{f}_{\text{curr}} \leftarrow h_{\text{next}}, \mathbf{f}_{\text{next}}$
- 12: **end if**
- 13: $T_{\text{acc}} \leftarrow \alpha_{\text{acc}} T_{\text{acc}}$, $T_{\text{size}} \leftarrow \alpha_{\text{size}} T_{\text{size}}$
- 14: **end for**
- 15: **end for**
- 16: $D_0 \leftarrow \text{SelectDiverseSubset}(I_A, n)$
- 17: **return** D_0

each objective, $f_k(h) \sim GP(\mu_k(h), k_k(h, h'))$, and proposing new candidates via an acquisition function such as Expected Hypervolume Improvement (EHVI): $h_{\text{next}} = \arg \max_h \alpha_{\text{EHVI}}(h)$.

The quality of the initialization set $D_0 = (h_i, f(h_i))_{i=1}^n$ is critical, as it determines the early posterior means and variances, thereby shaping the exploration trajectory. Space-filling designs such as Latin Hypercube Sampling (LHS) or Sobol sequences provide uniform coverage of \mathcal{H} but, as summarized in Table I, they overlook the Pareto structure in the objective space.

To address this, we propose OASI, a simulated annealing-based method that generates a Pareto-biased initial archive visualized in Figure 2. OASI employs a MOSA [10]-inspired scheme of short stochastic chains (40–50 iterations). Each chain begins from a random solution h_{curr} and explores a perturbed neighbor h_{next} , evaluated on accuracy $A(h)$ and size $S(h)$. Acceptance is probabilistic: $p_{\text{acc}} = 1$ if $A(h_{\text{next}}) > A(h_{\text{curr}})$, else $\exp(-(A(h_{\text{curr}}) - A(h_{\text{next}}))/T_{\text{acc}})$; and $p_{\text{size}} = 1$ if $S(h_{\text{next}}) < S(h_{\text{curr}})$, else $\exp(-(S(h_{\text{curr}}) - S(h_{\text{next}}))/T_{\text{size}})$. A candidate is accepted only if $u_{\text{acc}} < p_{\text{acc}}$ and $u_{\text{size}} < p_{\text{size}}$, with $u_{\text{acc}}, u_{\text{size}} \sim \mathcal{U}(0, 1)$. Accepted moves update h_{curr} , while all evaluations are stored in the initializer archive I_A .

After all chains complete, D_0 is selected from I_A using a maximin rule to ensure broad coverage of \mathcal{H} . This objective-aware initialization reduces surrogate bias, accelerates convergence, and improves MOBO’s sample efficiency under TinyML constraints. The complete procedure is summarized in Algorithm 2.

IV. EXPERIMENT AND RESULT

We evaluate on the Google Speech Commands v2 (GSC) corpus [11], using 10 balanced classes (8k train, 1k validation, 1k test each). All clips are normalized to 1.0 s at 16 kHz and converted into 40-bin log-Mel spectrograms (25 ms window, 10 ms hop). As

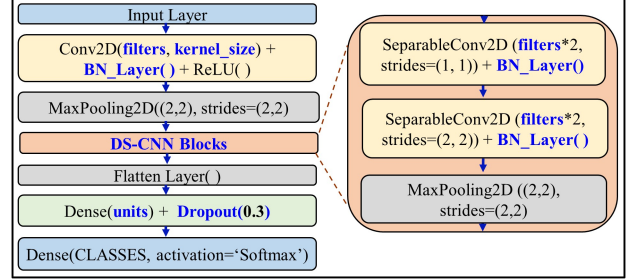


Fig. 3: A general architecture of the DSCNN highlighting the key hyperparameters used in this work.

the backbone, we adopt a depthwise separable CNN (DS-CNN) [7] shown in Figure 3, where standard convolutions are factored into a lightweight spatial filter followed by a pointwise projection, greatly reducing parameters and multiply-accumulate operations while preserving accuracy—making DS-CNNs highly suitable for TinyML and low-latency embedded inference. The hyperparameter search space is restricted to balance accuracy and efficiency: convolutional layers 1, 2, 3, filters 16–64, kernel sizes (3, 3), (5, 5), fully connected layers 1, 2, 3, with batch normalization and dropout as options. Implementation used Python 3.12.7, TensorFlow 2.14.0, and Librosa 0.10.1. Models were trained with Adam ($\text{lr} = 10^{-3}$, $\beta_1 = 0.9$, $\beta_2 = 0.999$), batch size 64, and up to 100 epochs with early stopping (patience 10) and checkpointing. Experiments ran on an NVIDIA RTX A4000 GPU with an Intel Xeon W-2245 CPU.

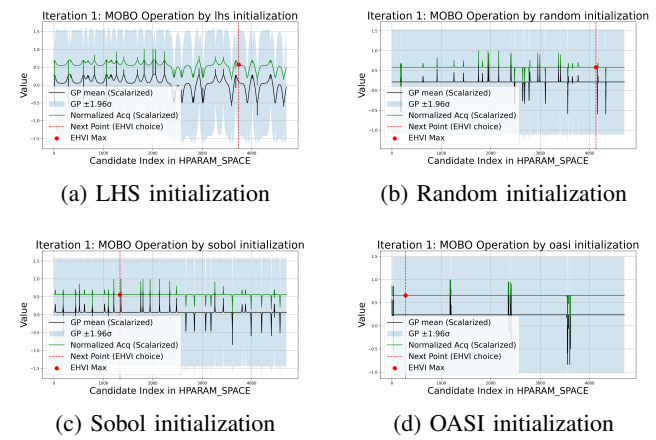


Fig. 4: Effect of initialization strategies on MOBO.

Fig. 4 shows how different initialization methods affect MOBO. LHS, Random, and Sobol spread points across the space but ignore the objectives, so the surrogate often starts with uninformative data. OASI, by contrast, uses MOSA to generate candidates guided by accuracy and size, giving the surrogate a stronger start and leading to better trade-offs under tight budgets. Fig. 5 shows the progression

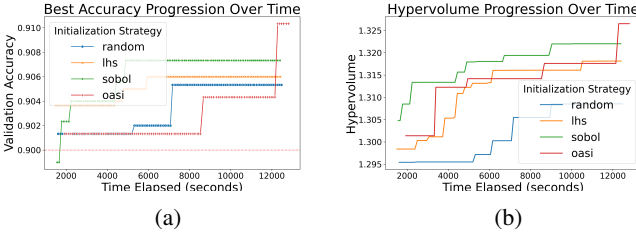


Fig. 5: Comparison of initialization strategies in terms of (a) best validation accuracy progression and (b) hypervolume progression over time.

TABLE II: Performance comparison of initialization strategies in terms of HV, GD, and computation time.

	Hypervolume (HV)	Generational Distance (GD)	Time (Sec.)
lhs	0.056336	0.462394	1501.79
random	0.056773	0.005563	1501.79
sobol	0.059255	0.003757	1562.11
oasi	0.062748	0	1934.88

of validation accuracy and hypervolume over time. OASI consistently outperforms LHS, Random, and Sobol, achieving higher accuracy and hypervolume from the start. This advantage comes from its objective-aware seeding, which supplies the surrogate with Pareto-relevant candidates early on, leading to faster convergence and sustained improvements.

Fig. 6a shows the combined objective $J(h)$ from Eq. 10, where lower values indicate better trade-offs between accuracy and size. OASI achieves and maintains the lowest J , reflecting the best accuracy-size trade-off; Sobol improves in steps but remains above OASI, LHS plateaus higher, and Random is consistently worst. The distribution in Fig. 6b further highlights OASI’s advantage, showing tighter spread and more reliable outcomes compared to the broader variability of LHS and Random.

Table II compares initialization methods by hypervolume (HV), generational distance (GD), and runtime. OASI yields the highest HV and lowest GD (zero), demonstrating superior convergence to the Pareto front, with only marginally higher runtime than others. A Kruskal-Wallis test [12] ($H = 5.40$, $p = 0.144$, $\eta^2 = 0.0007$) and Dunn’s post-hoc analysis (as illustrated in Table III) confirmed no significant differences at $\alpha = 0.05$, but OASI still showed consistently stable results.

Finally, Table IV lists top Pareto-front models found via Tchebycheff scalarization. OASI (rank 1) delivers the best trade-off, achieving >90% accuracy with the smallest size (0.10 MB) and lowest FLOPs/MACs. Sobol and LHS reach slightly higher accuracy (up to 0.904) but require larger models (~ 0.11 MB) and 3–4× higher FLOPs/MACs, making them less practical for TinyML deployment.

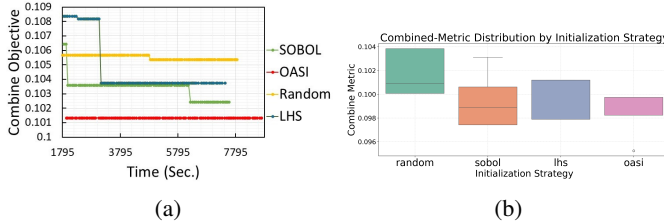


Fig. 6: (a) Combined objective over time for different initialization strategies and (b) Distribution of the combined objective across different initialization strategies.

TABLE III: Dunn’s test (Holm-adjusted p-values)

	oasi	lhs	random	sobol
oasi	1.000	0.705	0.000	0.917
lhs	0.705	1.000	0.000	0.705
random	0.000	0.000	1.000	0.000
sobol	0.917	0.705	0.000	1.000

TABLE IV: Model Performance Metrics

Rank	Model	Accuracy	Size (MB)	FLOPs	MACs
1	oasi_0	0.901333	0.103981	2518236	1259118
2	lhs_56	0.901000	0.109226	5132386	2566193
3	sobol_79	0.900000	0.104820	2936500	1468250
4	sobol_6	0.904000	0.111187	7968374	3984187
5	lhs_30	0.904000	0.111458	8151020	4075510

V. CONCLUSION

OASI consistently improves initialization for MOBO in TinyML KWS, achieving the highest hypervolume (0.0627) and lowest generational distance (0.0) compared to LHS, Sobol, and Random. While statistical tests (Kruskal-Wallis: $H = 5.41$, $p = 0.144$, $\eta^2 = 0.0007$) show that differences are not always significant, OASI provides more reliable convergence toward the Pareto front. It also yields favorable size-accuracy trade-offs (e.g., > 90% accuracy with < 200k parameters), crucial for strict TinyML resource budgets. The results highlight that objective-aware initialization has a decisive role to play in Bayesian optimization and verify OASI as an effective framework for constrained multi-objective optimization. Though implemented with KWS as a test platform, the technique applies to the majority of TinyML applications where classification accuracy is to be balanced with memory, latency, and energy.

REFERENCES

- [1] I. López-Espejo, Z.-H. Tan, J. H. Hansen, and J. Jensen, “Deep spoken keyword spotting: An overview,” *IEEE Access*, vol. 10, pp. 4169–4199, 2021.
- [2] P. Warden and D. Situnayake, *Tinyml: Machine learning with tensorflow lite on arduino and ultra-low-power microcontrollers*. O’Reilly Media, 2019.
- [3] S. Garai and S. Samui, “Exploring tinyml frameworks for small-footprint keyword spotting: A concise overview,” in *2024 International Conference on Signal Processing and Communications (SPCOM)*. IEEE, 2024, pp. 1–5.
- [4] L. Greif, N. Hübschle, A. Kimmig, S. Kreuzwieser, A. Martenne, and J. Ovtcharova, “Structured sampling strategies in bayesian optimization: evaluation in mathematical and real-world scenarios,” *Journal of Intelligent Manufacturing*, pp. 1–31, 2025.
- [5] M. Stein, “Large sample properties of simulations using latin hypercube sampling,” *Technometrics*, vol. 29, no. 2, pp. 143–151, 1987.
- [6] A. Dinno, “Nonparametric pairwise multiple comparisons in independent groups using dunn’s test,” *The Stata Journal*, vol. 15, no. 1, pp. 292–300, 2015.
- [7] S. Garai and S. Samui, “Advances in small-footprint keyword spotting: A comprehensive review of efficient models and algorithms,” *arXiv preprint arXiv:2506.11169*, 2025.
- [8] M. Renardy, L. R. Joslyn, J. A. Millar, and D. E. Kirschner, “To sobol or not to sobol? the effects of sampling schemes in systems biology applications,” *Mathematical biosciences*, vol. 337, p. 108593, 2021.
- [9] S. Daulton, D. Eriksson, M. Balandat, and E. Bakshy, “Multi-objective bayesian optimization over high-dimensional search spaces,” in *Uncertainty in Artificial Intelligence*. PMLR, 2022, pp. 507–517.
- [10] S. Bandyopadhyay, S. Saha, U. Maulik, and K. Deb, “A simulated annealing-based multiobjective optimization algorithm: Amosa,” *IEEE transactions on evolutionary computation*, vol. 12, no. 3, pp. 269–283, 2008.
- [11] P. Warden, “Speech commands: A dataset for limited-vocabulary speech recognition,” *arXiv preprint arXiv:1804.03209*, 2018.
- [12] H.-Y. Kim, “Statistical notes for clinical researchers: Nonparametric statistical methods: 1. nonparametric methods for comparing two groups,” *Restorative dentistry & endodontics*, vol. 39, no. 3, p. 235, 2014.